Heliyon 9 (2023) e16829

Contents lists available at ScienceDirect

Heliyon

journal homepage: www.cell.com/heliyon

Assessing short- and long-term modifications of steady-state water infiltration rate in an extensive Mediterranean green roof

C. Bondì [a], P. Concialdi [a], M. Iovino [a,*], V. Bagarello [a,b]

[a] Dipartimento di Scienze Agrarie Alimentari e Forestali, Università degli Studi di Palermo, Italy
[b] Centro Interdipartimentale di Ricerca "MIGRARE. Mobilità, differenze, dialogo, diritti", Università degli Studi di Palermo, Italy

ARTICLE INFO

Keywords:
Infiltration
Growing medium
Green roof
Detention capacity
Minidisk Infiltrometer

ABSTRACT

Green roof detention capacity is related to the steady-state infiltration rate, i_s, of the growing medium. With the aim to investigate short- and long-term modifications of the detention capacity of an extensive Mediterranean green roof, three mini-disk infiltrometer (MDI) measurement campaigns were conducted at construction, after one season and after five years of operation. A laboratory experiment was designed to separately measure i_s in the upper and the lower part of the substrate profile. During the first operating season, field i_s increased by a factor of 2.4 and 1.9 for near-saturated (applied pressure head, $h_0 = -30$ mm) and quasi-saturated conditions ($h_0 = -5$ mm), respectively. Similar rainfall height did not induce significant modifications in the upper layer of the laboratory columns, even if contribution of small pores to water infiltration tended to increase. Differently, i_s significantly decreased by a factor of 3.4–5.3 in the lower layer. After the simulated rainfall, the upper layer was less packed (mean bulk density, $\rho_b = 1.083$ kg m^{-3}) and the lower layer was more packed ($\rho_b = 1.218$ kg m^{-3}) as compared with the initial density ($\rho_b = 1.131$ kg m^{-3}) and the lower part enriched in small particles. Short-term modifications in the experimental plot were thus attributed to fine particles washing-off and bulk density decrease in the upper layer, yielding an overall more conductive porous medium. After five years of green roof operation, field i_s did not further increase thus showing that the washing/clogging mechanism was complete after one season or it was masked by counteracting processes, like root development and hydrophobicity.

1. Introduction

Green roof hydrological performance depends on the water retention capacity, i.e. the rainfall volume stored by the growing medium that is lost via evapotranspiration, and the detention of runoff, i.e. the transient storage of rainfall which reduces and delays the peak outflow rate [1,2]. Control of green roof detention properties is required to reduce the risks associated with pluvial flooding and/or combined sewer overflows. However, detention process is difficult to characterize as it combines the effects of plant, substrate and drainage layers as well as their interactions [3].

For the scopes of stormwater management, it is generally assumed that the potential of a green roof to retain and detain runoff remains constant over time. However, similarly to other natural or artificial porous media, the growing substrate may undergo temporal changes due to various biological and physical processes [3]. Root growth can reduce pore volumes due to local compaction

* Corresponding author.
E-mail address: massimo.iovino@unipa.it (M. Iovino).

https://doi.org/10.1016/j.heliyon.2023.e16829
Received 28 March 2023; Received in revised form 30 May 2023; Accepted 30 May 2023
Available online 2 June 2023

and pore filling [4,5]. The decay of dead roots leaves channels which may increase pore spaces and act as flow paths, increasing hydraulic conductivity [6]. Accumulation of suspended solids on the surface or in the void spaces of the porous media is responsible for clogging that reduces infiltration capacity [7,8]. Self-filtration, i.e., the process of particle mobilization and re-deposition within the porous medium, may result in a more compacted and less conductive lower layer [9].

Despite it can be expected that the age of green roof would influence hydraulic performances, specific studies are limited mainly because natural climatic variations tend to mask any subtle changes in the underlying hydrological characteristics of the system [10]. Getter, Rowe and Andresen [11] found that the pore volume doubled (from 41 to 82%) and the water-holding capacity increased from 17 to 67% after five years of usage. However, a review of data from 18 studies did not show any significant effect of green roof age on the annual runoff volume [12]. Seasonal variations of the detention performance of three different substrates were found to be more evident than annual trends due to time variable hydrophobicity of the substrate [13].

According to the conceptual model for green roof detention proposed by Kasmin, Stovin and Hathway [14], runoff occurs only when the field capacity of the substrate is exceeded. Thus, detention is basically controlled by the gravity driven flow through the interconnected larger pores of the growing medium that occurs for moisture content close to saturation. Monitoring the substrate steady-state infiltration rate under saturated or near-saturated conditions is therefore a potentially valuable tool for assessing modifications of detention capacity due to aging.

A relatively easy, rapid and inexpensive measurement of infiltration rate with a minimal disturbance of surface layer can be conducted by the MiniDisk Infiltrometer (MDI) [15]. Furthermore, field infiltration methods maintain functional connection of the conductive pore system with the surrounding medium [16]. Application of MDI allowed to investigate the seasonal variation in saturated and near-saturated hydraulic conductivity of the growing substrate of an extensive green roof plot established at the University of Palermo [17]. After only one growing season, the saturated hydraulic conductivity increased by a factor of 1.4 and the near-saturated hydraulic conductivity by a factor 3.0 compared to the initial values estimated on the new substrate at the time of green roof construction. The main cause of the observed differences was attributed to washing off of fine particles that accumulated in the lower layer. However, measurements of hydraulic conductivity in the lower layer of the growing medium were not conducted and the role of washing/clogging process was hypothesized on the basis of the observed modifications in particle size distribution and substrate bulk density.

This study was conducted to fill the gap of knowledge on the processes underlying the short-term modifications of green roof detention capacity. A laboratory MDI experiment was designed to detect modifications in steady-state infiltration characteristics of the growing substrate as a consequence of particle self-filtration operated by rainfall. Laboratory data were compared with field data obtained by Alagna, Bagarello, Concialdi, Giordano and Iovino [17] during the first year of operation of the extensive green roof plot. Furthermore, with the aim to investigate green roof aging at a longer temporal scale, in-situ MDI tests were replicated in the same full scale plot after five years of operation.

2. Materials and methods

2.1. Field experiments

The extensive green roof experimental plot at the Department of Agricultural, Food and Forest Sciences of University of Palermo is planted with *Sedum sediforme* and covers a plane surface of 18 m^2 (3 m wide by 6 m long). The green roof was constructed with the

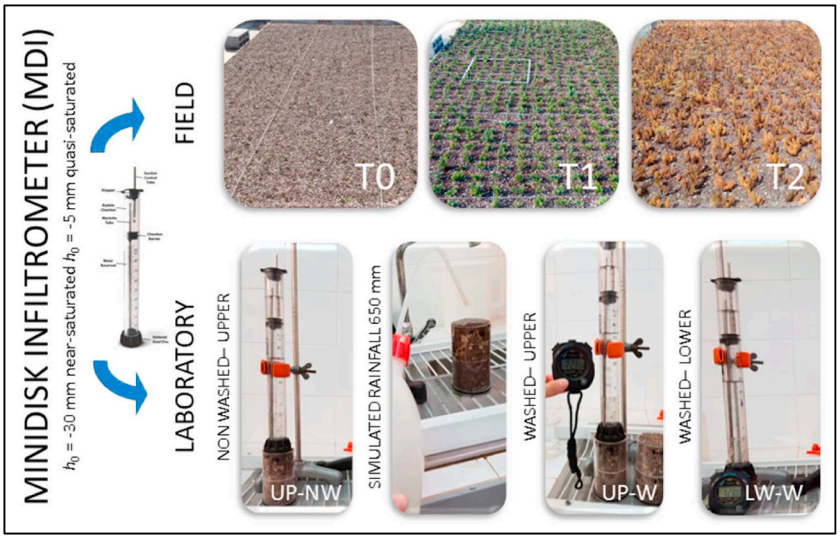

Fig. 1. Experimental setup.

"Mediterranean green roof system" supplied by HARPO Verdepensile (Trieste, Italy) that consists of a 3-cm-thick drainage and accumulation layer and a growing substrate (approximately 8 cm high) made by a mixture of 80% mineral fraction (lapillus, pumice and zeolite) and 20% organic fraction (peat and compost). According to the technical specifications released by the manufacturer, substrate dry bulk density, ρ_b, is 850–1000 kg m^{-3}, saturated hydraulic conductivity, K_s, is larger than 1200 mm/h and field capacity (i.e., water content at 100 cm suction), θ_{fc} = 0.30–0.45 m^3m^{-3}.

Field infiltration experiments were conducted at the surface of the experimental plot in December 2017 (T0), at the time of green roof construction, and then in October 2018 (T1) at the end of the first growing season [17]. In summer 2022, i.e. after five years of green roof operation, the experimental plot was sampled again (T2), following the same experimental procedure, to assess long-term variations of the infiltration characteristics. A Minidisk Infiltrometer (MDI) manufactured by Decagon (Decagon Devices, Inc., Pullman, WA) having a disk diameter of 4.5 cm was applied by imposing pressure head, h_0, values of −30 and −5 mm (Fig. 1). The former value of h_0 was established to explore near-saturated conditions given that, according to the capillary law, only pores having an equivalent diameter, d_e, smaller than approximately 1 mm contribute to water flow whereas larger pores are empty. The latter value of h_0 was set to explore saturated (or quasi-saturated) conditions. A slight negative value of h_0 was selected to exclude the artefact due to porous plate resistivity on the assessment of infiltration rate when h is set to zero. In theory, a value of $h_0 = -5$ mm activates pores with equivalent diameter up to 6 mm therefore allowing assessment of substrate transmission properties closely related to the saturated condition. At each sampling date, 18 randomly selected sites were sampled for each of the two considered h_0 values. The surface layer of the experimental plot was also sampled at each measurement site to determine the initial gravimetric water content, U_i (g g^{-1}), after oven-drying at 105 °C for 24 h.

During time interval between T0 and T1, 638 mm rainfall occurred that is very close to the average year precipitation for the area of Palermo (from 637 to 755 mm in the period 2002–2018, depending on the rain gauge location). From T1 to T2, 1432 mm rainfall occurred mainly concentrated in fall-winter months. During the considered time interval (T0 - T2), no irrigation was performed and the vegetation was fed only by natural rainfalls.

For each of 108 infiltration experiments forming the considered dataset (18 locations x 2 pressure heads x 3 campaigns), the steady-state infiltration rate, i_s (mm h^{-1}), was estimated from the slope of the regression line fitted to linear portion of the cumulative infiltration, I (mm), vs. time, t (s), curve. A minimum of five consecutive I vs. t data was considered for regression and the maximum relative error between the estimated and measured I values in the linear portion of the infiltration curve was calculated.

2.2. Laboratory experiments

Nine soil columns were prepared by packing new substrate into plexiglass tubes (internal diameter, D = 5.5 cm; height L = 10 cm) made by two separate halves to split the soil sample into an upper (UP, 0–5 cm depth) and a lower (LW, 5–10 cm depth) part. A wire mesh (diameter 0.5 mm) and a nylon cloth was put at the bottom of the column to replicate a lower boundary condition similar to that of the experimental plot. The sample preparation was conducted following a repeatable procedure that consisted in filling the tube in four successive layers (each approximately 2.5 cm high) and compacting the sample by tapping it 10 times from a height of 2–3 cm. The mean dry bulk density (ρ_b = 1.13 g/cm^3, CV = 5.47%) was larger but not far from the one reported for the full scale green roof by Alagna, Bagarello, Concialdi, Giordano and Iovino [17].

Infiltration tests were performed by a MDI at the same imposed pressure heads of −5 mm and −30 mm at the soil surface. A small amount of 2-mm sieved substrate was spread onto the sample surface to fill the small depression and ensure a full hydraulic contact between the porous plate and the infiltrating surface. Given the dimension of the infiltration source was very close to the sample diameter, the hypothesis of one-dimensional (1D) water flow into the substrate was assumed. Water flow under laboratory conditions was therefore different form the field one. In the latter, a three-dimensional (3D) flux is expected due to the contribution of lateral capillarity as a consequence of unconfined infiltration [16]. However, the use of 1D infiltration experiments seemed appropriate as, under field conditions, the hypothesized self-filtration process activated by rainfall is a vertical process.

Similarly to field experiments, the steady-state infiltration rate, i_s (mm h^{-1}), was determined from the slope of the linear regression line fitted to $I(t)$ data. A minimum of five consecutive I vs. t data was considered for regression and the maximum relative error between the estimated and measured I values in the linear portion of the infiltration curve was calculated.

To simulate the effect of particle washing off operated by rainfalls, the following experimental procedure was followed (Fig. 1). After sample preparation, a first MDI run was performed on the sample surface with the pressure head $h_0 = -30$ mm applied first and $h_0 = -5$ mm after 24 h redistribution (non-washed columns, NW). The soil columns were then washed with 1500 cm^3 water applied in three steps of 500 cm^3 in three consecutive days to simulate the effect of a cumulative rainfall height of 650 mm, that is very close to the total rainfall amount recorded between T0 and T1. Soil columns were allowed to dry under laboratory conditions until an initial soil water content value close to the initial one was reached. A second MDI run was performed on the sample surface with the pressure head $h_0 = -30$ mm applied first and $h_0 = -5$ mm after 24 h redistribution (washed columns, W). Then, the soil columns were disassembled and dried to the same initial soil moisture content under laboratory conditions. A third MDI run was conducted on the surface of the lower part on the column following the same procedure (i.e., infiltration at $h_0 = -30$ mm followed by infiltration at $h_0 = -5$ mm after 24 h redistribution). Soon after the end of the MDI experiments, the upper (UP) and the lower (LW) parts of the soil columns (each having a thickness of 5 cm) were weighted and dried at 105 °C to determine final soil gravimetric water content and bulk density. Crushed samples were then sieved through a series of eight sieves (9.53, 6.0, 5.0, 4.0, 2.8, 2.0, 0.85, 0.25 mm) and the particle size distribution of both the total and the UP and LW parts of the columns determined.

2.3. Statistical analyses

The statistical frequency distribution of i_s data obtained from field and laboratory experiments was checked with the Lilliefors [18] test ($P = 0.05$), considering both a normal (NO) and a ln-normal (LN) distribution. For the field dataset, both the NO and LN distribution hypotheses were rejected for the second sampling date (T1) independently of the applied pressure head value. The LN distribution hypothesis was also rejected for experiments conducted at $h_0 = -30$ mm at third sampling date (T2). Therefore, the non-parametric Mann-Whitney U test [19] was applied to compare i_s data collected at the different field sampling dates ($P = 0.05$). A pairwise approach was applied to establish comparisons between i_s data in accordance with other investigations focused on sampling soil properties at different dates [20].

Both the NO and LN distribution hypothesis were never rejected for the steady-state infiltration rate collected at the two applied pressure heads on the laboratory repacked soil columns. Statistics of i_s were therefore calculated according to a NO distribution. Comparison between mean i_s values collected in the UP part of the column before and after simulated rainfall and between UP and LW parts of the column after water treatment were therefore conducted according to a paired t-test ($P = 0.05$).

A NO distribution was also assumed for U_i values measured at the three sampling dates in the experimental plot and statistical comparisons conducted by F-test and unpaired two-tailed t-test ($P = 0.05$).

3. Results and discussion

3.1. Field experiments

The experimental plot was sampled under different conditions of initial gravimetric water content (Table 1). The lowest mean U_i was measured for the summer sampling (T2) whereas the highest value corresponded to the T1 sampling that was conducted in October a few days after 40.8 mm rainfall occurred. Fall sampling was also characterized by the lowest spatial variability of U_i values. The winter (T0) and fall (T1) samplings showed similar maximum and minimum values but means differed by a factor of 1.36. It is worth noting that the maximum initial substrate water content in summer ($U_i = 0.019$ g g^{-1}) is far below the minimum value measured for the former two campaigns ($U_i = 0.136$ and 0.153 g g^{-1} for T0 and T1, respectively) thus showing the very dry conditions that may occur in the growing substrate during the summer season. The relatively high variability of U_i is line with the general guidelines proposed by Warrick [21] and other field investigations conducted on natural soils (e.g., Refs. [22,23]). However, further investigations need to be conducted to assess if the sampled substrate volume at each site (approximately 200 cm^3) can be considered representative for estimating the moisture content in heterogeneous media characterized by a large coarse fraction (52.3% by mass of particles were larger than 9.53 mm in size).

Independently of the sampling date, infiltration tests conducted at $h_0 = -30$ mm were on average 2.75 times longer than the corresponding tests conducted at $h_0 = -5$ mm. Following the theory, the infiltration rate was generally maximum at the initial stage of infiltration and then approached a steady-state condition [16]. A clear detection of a steady-state phase was always possible as showed by the single R^2 values that were always greater than 0.9848 (mean R^2 values equal to 0.9993 and 0.9992 for $h_0 = -5$ and -30 mm, respectively) and the low values of E_{max} (mean E_{max} equal to 1.2% and 1.5% for $h_0 = -5$ and -30 mm, respectively). Bagarello, Iovino and Reynolds [24] assumed a relative error of 2% between estimated and measured cumulative infiltration as a criterion to establish the onset of the steady-state stage but values up to 5% were considered acceptable [25]. In this investigation, the threshold of 2% was exceeded in 21 out of 108 experiments and the threshold of 5% never exceeded. Therefore, steady-state unconfined infiltration flux was always achieved during the experiments. Due to contribution of the pores with $d_e > 1$ mm, the mean steady-state infiltration rate for quasi-saturated conditions ($h_0 = -5$ mm) was on average 4.8 times larger than under near-saturated ($h_0 = -30$ mm) conditions.

For 3D infiltration into homogeneous soil, i_s depends on both soil hydraulic conductivity and sorptivity [26]. The former controls gravity flow whereas the latter, that depends on the initial soil water content, accounts for lateral expansion of the wetted bulb due to capillarity. The relative influence of the gravity over capillary flow can be detected from the shape of the cumulative infiltration curve, $I(t)$, in the initial transient stage on the infiltration process. A downward concavity indicates that the process is influenced by capillarity whereas a $I(t)$ curve that is linear with time indicates that the process is mainly driven by gravity, with limited or no influence of capillarity [16], and is therefore essentially 1D. An upward concavity of the $I(t)$ curve can occur in particular cases as for infiltration in water repellent soils [27–29]. In order to establish a comparison between field and laboratory infiltration tests, the influence of lateral capillary flow on the field measured infiltration process was preliminarily assessed by calculating the ratio between the mean

Table 1
Statistics of initial gravimetric water content, U_i (g g^{-1}), measured at the green roof plot for the different sampling dates.

	T0	T1	T2
N	18	18	18
min	0.136	0.153	0.007
max	0.304	0.316	0.019
mean	0.178 b	0.234 c	0.012 a
CV	23.3	14.7	25.4

Values followed by the same letter are not significantly different ($P = 0.05$).

infiltration rate, i_m, and the steady-state infiltration rate, i_s. An i_m/i_s ratio close to one identifies a cumulative infiltration curve that is linear with time. An $i_m/i_s > 1$ identifies a downward concavity whereas $i_m/i_s < 1$ an upward concavity.

The i_m/i_s ratio ranged from 0.94 to 1.39 with a mean value of 1.16 for the lower applied pressure head value ($h_0 = -30$ mm) and from 0.90 to 1.48 with a mean value of 1.14 for $h_0 = -5$ mm (Fig. 2). For a given sampling date, the set of i_m/i_s values collected under near-saturated and quasi-saturated conditions were not significantly different thus indicating that, under similar initial water content, the contribution of capillarity was not influenced by the applied pressure head. For both near-saturated and quasi-saturated conditions, Fig. 3 shows the normalized cumulative infiltration (I at any given time/cumulative infiltration at the end of the run, I_f) curves corresponding to the maximum (downward concavity) and the minimum (upward concavity) i_m/i_s values. The case of an infiltration curve with $i_m/i_s = 1$ (i.e., $I(t)$ curve linear on average) is also showed.

No i_m/i_s value lower than 1.0 was observed for the first two sampling dates (T0 and T1) (Fig. 2) and the slope of the regression line between i_m/i_s and U_i was not significantly different from zero, thus confirming that the initial moisture contents did not influence the contribution of lateral capillary flux for $U_i > 0.13$ g g^{-1}. Overall, the i_m/i_s values close to one indicate that the concavity of the measured infiltration curve was generally moderate and most of the infiltration curves showed steady-state conditions from the very beginning of the run. It was concluded that the lateral capillary flow had limited influence on the steady infiltration flux under unconfined field conditions. The steady-state infiltration rate can be therefore considered mainly dominated by gravity flow thus making it reasonable to compare the field MDI 3D tests conducted during the first operating season (T0 and T1 sampling dates) and the laboratory MDI 1D tests on repacked columns.

At the time of green roof construction (T0), the median steady-state infiltration rate was 37.5 mm/h under near-saturated conditions ($h_0 = -30$ mm) with an interquartile range (IQR) of 0.1 mm/h. For quasi-saturated conditions ($h_0 = -5$ mm), a median $i_s = 147.8$ mm/h was detected with an IQR of 35.2 mm/h (Table 2). Assuming the ratio between IQR and median value as a measure of the relative spatial variability of i_s, it was 0.003 at $h_0 = -30$ mm and 0.452 at $h_0 = -5$ mm. Field MDI experiments thus showed that initial packing of substrate resulted in a highly uniform distribution of pores with equivalent diameter, d_e, lower than 1 mm whereas relative spatial variability of larger pores ($d_e > 1$ mm) was two orders of magnitude higher. As documented by Alagna, Bagarello, Concialdi, Giordano and Iovino [17], following one operating season (T1), the steady-state infiltration rate significantly increased by a factor of 2.4 at $h_0 = -30$ mm and a factor of 1.9 at $h_0 = -5$ mm. Spatial variability increased for both small pores (IQR to median ratio = 0.395) and large pores (IQR to median ratio = 0.548). Therefore, during the first ten months following construction, the active pores underwent a rearrangement that yielded a more conductive growing substrate with increased spatial variability. Increased infiltration capacity for both near- and quasi-saturated conditions is expected to affect the detention capacity of the green roof as rainfall will flow more rapidly through the growing medium with increased outflow peak rate and reduced delay between rainstorm and runoff.

The field campaign conducted after five operating seasons yielded a median i_s value of 51.9 mm/h under near-saturated conditions ($h_0 = -30$ mm) and 267.7 mm/h under quasi-saturated conditions ($h_0 = -5$ mm) (Table 2). Compared to the values collected at the end of the first growing season (T1), median infiltration rate significantly decreased by a factor of 1.71 at $h_0 = -30$ mm but was practically unaffected under quasi-saturated conditions (i.e., i_s decreased by a not significantly factor of 1.02). At T2 sampling date, the maximum spatial variability of the considered monitoring period was observed, with a ratio between IQR and median values of i_s equal to 0.943 and 0.715 for $h_0 = -30$ and -5 mm, respectively (Fig. 4).

At $h_0 = -30$ mm, the long-term (T2) median i_s value was intermediate between the initial (T0) and the short-term (T1) median values. However, the maximum i_s at T2 was close to the maximum i_s value observed at T1 and around 28% of the i_s data collected at T2 were lower than the minimum value observed at T0 (Fig. 3). At $h_0 = -5$ mm, the long-term (T2) and short-term (T1) median i_s values coincided and 22% of long-term i_s data were higher than the maximum value observed at the end of the first operating season. In summary, long-term modifications increased variability but did not increased the average infiltration rate of the growing substrate as could be expected if the washing off process suggested by Alagna, Bagarello, Concialdi, Giordano and Iovino [17] had continued to

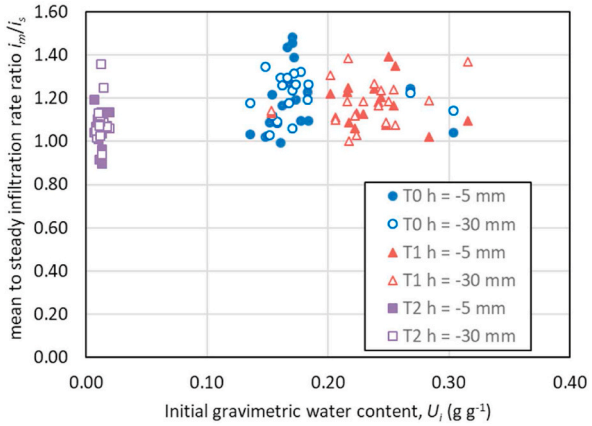

Fig. 2. Ratio between the mean infiltration rate and the steady-state infiltration rate, i_m/i_s, vs. initial gravimetric moisture content, U_i, of the experimental plot for field experiments conducted at the two pressure head values ($h_0 = -30$ and -5 mm).

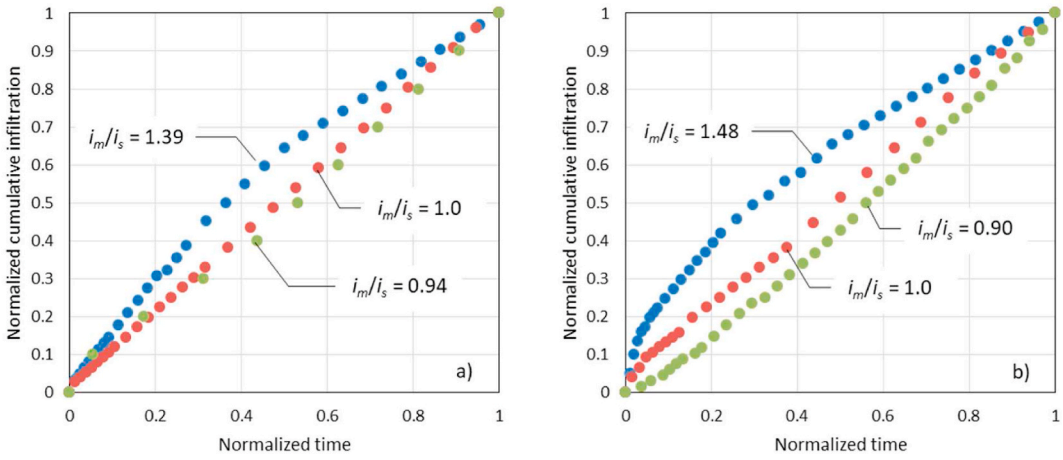

Fig. 3. Examples of normalized cumulative infiltration (I/I_f) curves corresponding to maximum, minimum and unity values of the ratio between the mean and the steady-state infiltration rates (I_f = cumulative infiltration corresponding to final time t_f); a) pressure head, $h_0 = -30$ mm, b) pressure head, $h_0 = -5$ mm.

Table 2
Statistics of steady-state infiltration rate, i_s (mm h^{-1}), for the different sampling dates and applied pressure heads.

	$h_0 = -30$ mm			$h_0 = -5$ mm		
	T0	T1	T2	T0	T1	T2
N	18	18	18	18	18	18
min	34.2	71.1	12.6	61.3	135.6	75.5
max	40.4	150.9	150.8	298.7	327.9	602.3
median	37.5 a	89.2 c	51.9 b	147.8 a	274.3 b	267.7 b
IQR	0.1	35.2	49.0	66.8	150.2	191.4

For a given pressure head value, values followed by the same letter are not significantly different ($P = 0.05$).

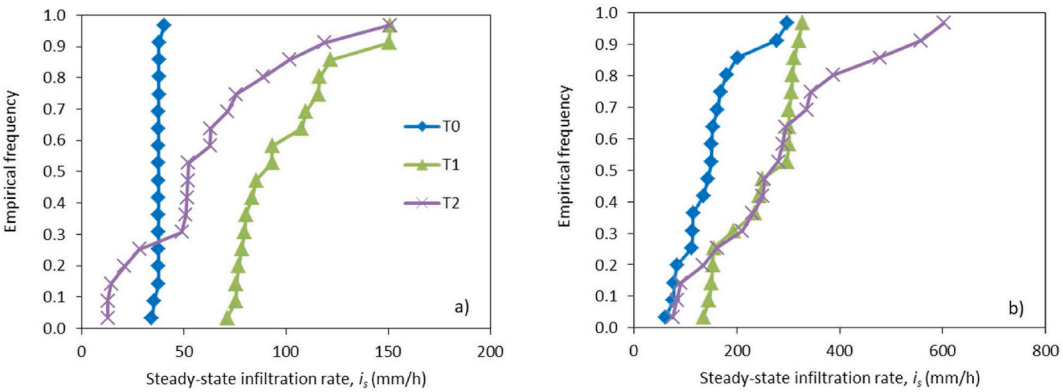

Fig. 4. Empirical frequency distributions of steady-state infiltration rate, i_s, determined at the two pressure head values ($h_0 = -30$ and -5 mm) for the three sampling dates; a) $h_0 = -30$ mm, b) $h_0 = -5$ mm.

operate in the spell from T1 to T2. The long-term detention capacity of the green roof is therefore relatively unaffected by aging and it should be expected that, following the decay of the first operating season, the hydrological performances will preserve with time. However, the increased heterogeneity of infiltration characteristics at T2 should be considered with caution given that, in specific spots of the vegetated roof, the detention properties could be severely jeopardized as a consequence of extremely high values of i_s under quasi-saturated conditions (Fig. 4).

Trying to explain the increased spatial variability of infiltration characteristics at T2, two possible phenomena could be invoked. One is the root growth that resulted in an uneven occlusion of conducting pores [5,30]. Another, is the onset of hydrophobicity due to vegetation exudates and decomposing materials [31,32]. Indeed, the characteristic upward concavity of the cumulative infiltration curve was observed only in four out of 36 infiltration runs conducted at T2 (Fig. 2). Both phenomena (i.e., root development and

hydrophobicity) can concur to reduce infiltration rate in smaller pores as they can be more easily occluded by roots and more affected by hydrophobicity than the large pores [33,34].

3.2. Laboratory experiments

The different initial water content of the soil columns affected the duration of the experiments. Near-saturated infiltration tests ($h_0 = -30$ mm) were conducted under substrate dry conditions as the initial gravimetric water content ranged from 0.019 to 0.024 g g^{-1} with a mean value of 0.022 g g^{-1} (coefficient of variation, CV = 5.47%). Average duration of the experiments was 1.35 h but a high variability was observed with a range between minimum and maximum duration of 4.10 h. Infiltration experiments at $h_0 = -5$ mm were conducted under much wetter conditions (mean $U_i = 0.342$, CV = 5.43%) and the total volume of the MDI reservoir (approximately 85 cm^3) took from 0.03 to 0.93 h to completely infiltrate into the soil column (mean duration 0.21 h). Independently of the applied pressure head at the column surface, a clear steady-state infiltration condition was always detected following a more or less prolonged transient stage. Coefficients of determination for the regression between measured and estimated $I(t)$ data were always greater than 0.9937 (mean $R^2 = 0.9986$). The average maximum relative error between the regression line and the measured I values was 2.1% and the threshold of 5% for E_{max} was exceeded only in two out of 54 infiltration experiments. The estimated i_s values can thus be considered representative of the steady-state 1D infiltration process in the repacked soil columns.

For both near-saturated ($h_0 = -30$ mm) and quasi-saturated ($h_0 = -5$ mm) conditions, the slope of the regression line between mean infiltration rate, i_m, and steady-state infiltration rate, i_s, was not different from unity ($P = 0.05$) and the mean ratio i_m/i_s was 1.24 and 1.22, respectively. Notwithstanding the different initial moisture content, the two mean i_m/i_s values were not statistically different thus confirming that the influence of capillarity was generally negligible for the substrate under study. The condition $i_m/i_s < 1$, indicating occurrence of hydrophobicity, was observed for a relatively high number of experiments (18 out of 54) mostly conducted under quasi-saturated conditions ($h_0 = -5$ mm). In particular, hydrophobic conditions ($i_m/i_s < 1$) were observed in 7 out of 9 experiments on non-washed (NW) samples.

The mean steady-state infiltration rate for the non-washed columns was 29.4 mm/h under near-saturated conditions (minimum $i_s = 1.9$ mm/h, maximum $i_s = 134.5$ mm/h) and 717.3 mm/h under quasi-saturated condition (minimum $i_s = 107.2$ mm/h, maximum $i_s = 1569$ mm/h) (Table 3). Increasing the surface pressure head from −30 to −5 mm thus determined, on average, more than one order of magnitude increase of the steady-state infiltration rate. Following simulated rainfall, the mean i_s increased by a factor of 1.50 at $h_0 = -30$ mm whereas it decreased by a factor of 1.25 for $h_0 = -5$ mm. In both cases differences were not significant.

Boxplot of i_s data estimated at $h_0 = -30$ mm for non-washed conditions (Fig. 5) highlighted the presence of an outlier, that is a single i_s data point that was more than twice the upper quartile value. When this outlier was disregarded, the mean i_s for UP-NW reduced to 16.3 mm/h and the difference between mean i_s values measured in the upper layer before and after washing resulted significant. Therefore, as a consequence of rainfall washing off, small pores contribution ($d_e < 1$ mm) tended to increase whereas large pores ($d_e > 1$ mm) contribution was practically unaffected (Fig. 5). This finding was not surprising given it is likely that prolonged leaching of samples mobilized the fine particles of the upper layer while the coarse ones, that are less mobile, remained in-situ. In agreement with this interpretation, variability of near-saturated i_s reduced (CV decreased from 141% to 87%) but remained almost the same for quasi-saturated i_s (Table 3).

Independently of the applied pressure head, after simulated rainfall the mean steady-state i_s of the bottom half of the columns was significantly lower than the upper one. The differences between the upper and the lower parts of the column were more pronounced for the experiments conducted under near-saturated conditions for which the steady-state infiltration rate decreased by a factor of 5.3 whereas under quasi-saturated conditions i_s decreased by a factor of 3.4. This result is also reasonable as it shows that small pores are more prone to the clogging phenomena determined by the fine particles washed off from the upper layer.

Seasonal modifications of green roof infiltration characteristics were more pronounced under field than laboratory conditions. In the time interval from T0 to T1, surface roof i_s increased by a significant factor of 1.9–2.4 depending on the applied pressure head (Table 2). Application of similar rainfall depth on the laboratory soil columns did not reveal significant changes in i_s or it suggested an increase on near-saturated i_s by neglecting a single data point (Table 3). Two counteracting factors likely contributed to the different findings for laboratory and field experiments: i) the mechanical compaction operated by rainfall; ii) the presence of plants. The total seasonal rainfall was applied in only three steps on laboratory soil columns thus promoting mechanical compaction of substrate that did not occur under natural rainfall. As a matter of fact, a small but significant change of ρ_b that increased from 1.13 to 1.15 kg m^{-3} (i.

Table 3
Statistics of steady-state infiltration rate for the upper (UP) and lower (LW) part of the substrate columns before (NW) and after the sample washing (W).

	near-saturated conditions $h_o = -30$ mm			quasi-saturated conditions $h_o = -5$ mm		
	UP–NW	UP–W	LW - W	UP–NW	UP–W	LW - W
N	9	9	9	9	9	9
min	1.9	6.2	2.5	107.2	150.4	15.2
max	134.5	129.7	24.3	1569.2	1265.7	384.3
mean	29.4 b	44.1 b	8.3 a	717.3 b	575.2 b	170.8 a
CV	140.7	86.6	78.3	75.8	69.8	90.8

For a given pressure head value, values followed by the same letter are not significantly different ($P = 0.05$).

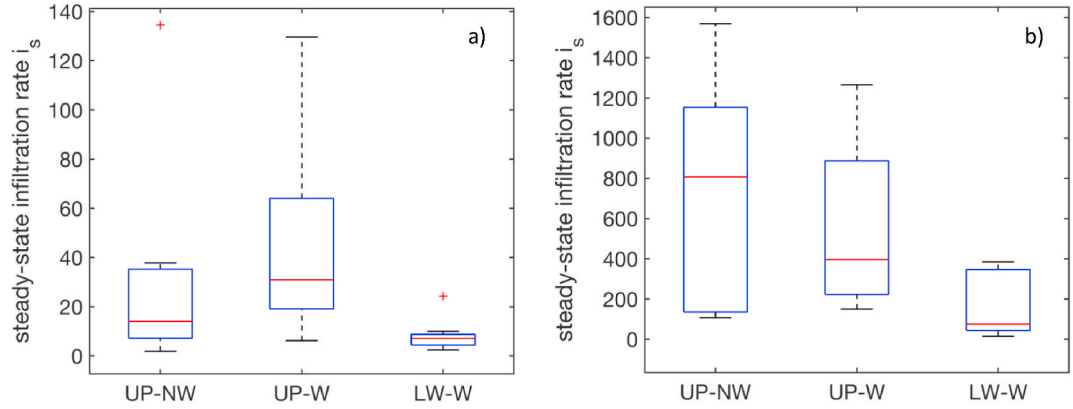

Fig. 5. Boxplot of steady-state infiltration rates collected for: a) near-saturated ($h_0 = -30$ mm) and, b) quasi-saturated ($h_0 = -5$ mm) conditions in the upper (UP) part of the columns before (NW) and after (W) simulated rainfall and in the lower (LW) part on the columns after simulated rainfall.

e., by a factor of 1.02) was observed for laboratory columns (Table 4). The substrate compaction, and the subsequent reduction of porosity, could have masked the effects of self-filtration thus yielding nearly stable or little variable i_s values in the upper layer of the columns. Conversely, under field conditions, plant canopy likely shielded the soil surface while roots contributed to maintain more conductive conditions in the upper layer of the growing media. Alagna, Bagarello, Concialdi, Giordano and Iovino [17] reported that the final bulk density of the upper layer was 0.85 times the bulk density at the time of roof construction thus showing that compaction due rainfall was not effective under field conditions. As a consequence, the self-filtration process was more effective in increasing the infiltration rates of field substrate.

Nevertheless, simulated rainfall modified the vertical distribution of substrate ρ_b with the upper layer of the soil column that was less compacted (mean $\rho_b = 1.083$ kg m^{-3}) and the lower layer that was more compacted (mean $\rho_b = 1.218$ kg m^{-3}) than the unwashed one (mean $\rho_b = 1.131$ kg m^{-3}) (Table 4). The observed changes in ρ_b were in agreement with changes in steady-state infiltration rate highlighting an increase of fine particle in the bottom layer and a decrease of fine particles in the upper layer.

Comparison of the relative proportions of the particles in a given texture class in the two halves of the columns (Fig. 6) showed that, after the simulated rainfall, the lower part of the sample enriched in small particles. Assuming that, for a given texture class, the initial vertical distribution of particle was uniform (i.e., 50% by weight of the particles in the upper part of the column and 50% in the lower part), the percentage of the fine particles tended to increase in the lower layer and decrease in the upper layer. This finding confirmed that the finest particles were mobilized from the upper layer and settled in the lower layer following the process referred to as self-filtration [9]. The phenomenon was particularly noticeable for particles with diameter smaller than 0.5 mm which likely were more mobile along the profile. For these fractions, the relative proportion in the lower layer increased up to 16%. Settling of fine particle determined phenomena of pore clogging in the lower layer of the soil columns that were considered the main cause of the observed reductions in steady-state infiltration rate.

4. Conclusions

Following artificial rainfall that mimicked the cumulative seasonal rainfall having occurred between the T0 and T1 sampling dates, the steady-state infiltration rate of the upper layer of the soil columns was not significant different from the initial one. In the field, the steady-state infiltration rate increased by a factor of 2.4 for near-saturated condition and by a factor of 1.9 for quasi-saturated condition. In agreement between the laboratory and the field experiments, signs were detected that, following simulated rainfall, contribution of small pores to water infiltration tended to increase as a consequence of prolonged leaching that mobilized the fine particles of the upper layer while the coarse ones, that are less mobile, remained in-situ.

A possible motivation of the observed differences between field and laboratory measurements of the upper layer i_s, may rely in the different combinations of compaction and self-filtration induced by natural and simulated rainfalls. Specifically, under field condition, plant canopy likely protected substrate surface, thus preventing compaction of the upper layer, and decay of dead roots improved the ability of the porous medium to transmit water. In this case, washing off of fine particles was particularly efficient in promoting the increase of porosity as confirmed by final bulk density (T1) that was 0.85 times the initial (T0) one. For laboratory columns, the two processes, i.e., mechanical compaction and washing of fine particles, played a counteractive role thus influencing the infiltration characteristics exclusively for the small pore system.

Simulated rainfall significantly affected the steady-state infiltration rates of the lower part of columns that were 3.4–5.3 times lower than the upper ones with larger reductions associated to the pore class that are activated for near-saturated condition ($d_e < 1$ mm). The hypothesized self-filtration process was confirmed by modifications in particle size distribution as the percentage of the fine particles tended to increase in the lower layer and decrease in the upper layer. It was concluded that rainfall can influence short-term infiltration characteristics of the green roof as a consequence of the detachment of fine particles from the top layer and clogging in the bottom layer. The detention properties of the green roof may be severely hampered as rainfall will flow more rapidly through the growing

Table 4
Statistics of the dry bulk density of the substrate columns before (NW) and after the simulated rainfall (W) and for the upper (UP) and lower (LW) parts following simulated rainfall.

	NW	W	UP-W	LW-W
N	9	9	9	9
min	1.025	1.059	0.994	1.091
max	1.227	1.243	1.174	1.320
mean	1.131 a	1.151 b	1.083 A	1.218 B
CV	5.47	4.94	6.89	6.68

Values followed by the same lowercase or uppercase letter are not significantly different ($P = 0.05$).

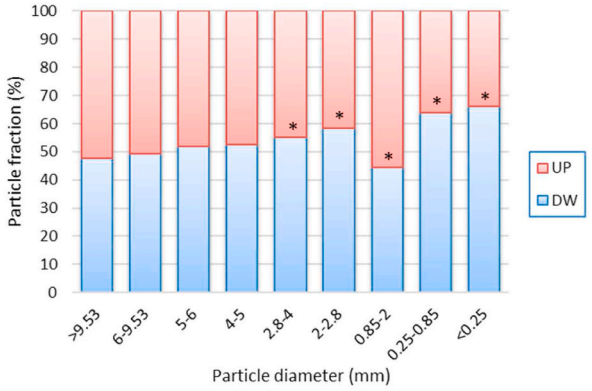

Fig. 6. Relative fractions of the particles in each considered diameter class after simulated rainfall.

medium due to increased steady-state infiltration rate close to saturation. Compared to the initial hydrological performance of the green roof, the outflow peak rate will be increased and delay between rainstorm and runoff reduced.

However, the field campaign conducted after five year of operation also showed that degradation of hydrological characteristics did not continue after the first growing season. Indeed, long-term modifications did not increase the average infiltration rate as could be expected if the self-filtration process had continued year after year. The lack of increases in i_s for quasi-saturated condition, or even the decrease for near-saturated one, was attributed to occlusion of small pores due to root development and onset of hydrophobicity due to vegetation exudates and decomposing materials. Uneven occurrence of both these phenomena explained the increased variability in infiltration characteristics.

Monitoring of infiltration characteristics is crucially important to detect modifications in green roof detention properties that could jeopardize most of their environmental benefits. Indeed, apart from the reduced ability to mitigate stormwater runoff, washing off of fine particle also reduces the retention properties of the growing medium thus hampering its ability to store water between two successive rainfalls. Therefore, plant water supply can be problematic for non-irrigated conditions. Also thermal properties of the vegetated roof may be affected with negative effects on building energy consumption. The simple and inexpensive MDI method proved to be effective in detecting both short- and long-term modifications of green roof hydrological properties directly in-situ and has the potential to be proposed as a routinely technique for temporal monitoring of aging phenomena that could compromise the benefits of the vegetated green infrastructures. A hydraulic characterization of the porous medium limited to its surface is not enough to properly describe its hydrological behaviour even if the thickness of the substrate is small.

Declaration of competing interest

The authors declare the following financial interests/personal relationships which may be considered as potential competing interests: Massimo Iovino reports financial support was provided by Government of Italy Ministry of Education University and Research. Vincenzo Bagarello reports financial support was provided by European Union Next-GenerationEU.

Acknowledgements

This study was carried out within the RETURN Extended Partnership and received funding from the European Union Next-GenerationEU (National Recovery and Resilience Plan – NRRP, Mission 4, Component 2, Investment 1.3 – D.D. 1243 August 2, 2022, PE0000005) and from Ministero dell'Istruzione, dell'Università e della Ricerca of Italy, project WATER4AGRIFOOD, contract "Tetto Verde", CON-0375, CUP B94I20000300005.

References

[1] Y. Li, R.W. Babcock Jr., Green roof hydrologic performance and modeling: a review, Water Sci. Technol. 69 (4) (2013) 727–738.
[2] V. Stovin, S. Poë, S. De-Ville, C. Berretta, The influence of substrate and vegetation configuration on green roof hydrological performance, Ecol. Eng. 85 (2015) 159–172.
[3] J. Czemiel Berndtsson, Green roof performance towards management of runoff water quantity and quality: a review, Ecol. Eng. 36 (4) (2010) 351–360.
[4] A.R. Dexter, Soil physical quality: Part I. Theory, effects of soil texture, density, and organic matter, and effects on root growth, Geoderma 120 (3) (2004) 201–214.
[5] K.M. Marcacci, J.M. Warren, E. Perfect, J.L. Labbé, Influence of living grass Roots and endophytic fungal hyphae on soil hydraulic properties, Rhizosphere 22 (2022), 100510.
[6] A. Schwen, G. Bodner, P. Scholl, G.D. Buchan, W. Loiskandl, Temporal dynamics of soil hydraulic properties and the water-conducting porosity under different tillage, Soil Tillage Res. 113 (2) (2011) 89–98.
[7] S. Le Coustumer, T.D. Fletcher, A. Deletic, S. Barraud, J.F. Lewis, Hydraulic performance of biofilter systems for stormwater management: influences of design and operation, J. Hydrol. 376 (1) (2009) 16–23.
[8] S. Lavrnić, V. Alagna, M. Iovino, S. Anconelli, D. Solimando, A. Toscano, Hydrological and hydraulic behaviour of a surface flow constructed wetland treating agricultural drainage water in northern Italy, Sci. Total Environ. 702 (2020), 134795.
[9] O. Dikinya, C. Hinz, G. Aylmore, Decrease in hydraulic conductivity and particle release associated with self-filtration in saturated soil columns, Geoderma 146 (1) (2008) 192–200.
[10] S. De-Ville, M. Menon, X. Jia, G. Reed, V. Stovin, The impact of green roof ageing on substrate characteristics and hydrological performance, J. Hydrol. 547 (2017) 332–344.
[11] K.L. Getter, D.B. Rowe, J.A. Andresen, Quantifying the effect of slope on extensive green roof stormwater retention, Ecol. Eng. 31 (4) (2007) 225–231.
[12] J. Mentens, D. Raes, M. Hermy, Green roofs as a tool for solving the rainwater runoff problem in the urbanized 21st century? Landsc. Urban Plann. 77 (3) (2006) 217–226.
[13] S. De-Ville, M. Menon, V. Stovin, Temporal variations in the potential hydrological performance of extensive green roof systems, J. Hydrol. 558 (2018) 564–578.
[14] H. Kasmin, V.R. Stovin, E.A. Hathway, Towards a generic rainfall-runoff model for green roofs, Water Sci. Technol. 62 (4) (2010) 898–905.
[15] V. Alagna, V. Bagarello, S. Di Prima, G. Giordano, M. Iovino, A simple field method to measure the hydrodynamic properties of soil surface crust, J. Agri. Eng. 44 (3s) (2013).
[16] R. Angulo-Jaramillo, V. Bagarello, M. Iovino, L. Lassabatere, Infiltration Measurements for Soil Hydraulic Characterization, Springer International Publishing, Cham, 2016, p. 383.
[17] V. Alagna, V. Bagarello, P. Concialdi, G. Giordano, M. Iovino, Evaluation of Green Roof Ageing Effects on Substrate Hydraulic Characteristics, Lecture Notes in Civil Engineering, 2020, pp. 89–97.
[18] H.W. Lilliefors, On the Kolmogorov-Smirnov test for normality with mean and variance unknown, J. Am. Stat. Assoc. 62 (318) (1967) 339–402.
[19] M.R. Spiegel, L.J. Stephens, Theory and Problems of Statistics, fourth ed. ed., McGraw-Hill, 2008.
[20] I. Mubarak, J.C. Mailhol, R. Angulo-Jaramillo, P. Ruelle, P. Boivin, M. Khaledian, Temporal variability in soil hydraulic properties under drip irrigation, Geoderma 150 (1–2) (2009) 158–165.
[21] A.W. Warrick, Appendix 1: spatial variability, in: D. Hillel (Ed.), Environmental Soil Physics, Academic Press, San Diego, CA, 1998, pp. 655–675.
[22] V. Bagarello, C. Di Stefano, M. Iovino, A. Sgroi, Using a transient infiltrometric technique for intensively sampling field-saturated hydraulic conductivity of a clay soil in two runoff plots, Hydrol. Process. 27 (24) (2013) 3415–3423.
[23] V. Bagarello, G. Caltabellotta, P. Concialdi, M. Iovino, Comparing two methods to perform a beerkan infiltration run in a loam soil at different dates, J. Hydrol. 617 (2023), 129095.
[24] V. Bagarello, M. Iovino, W.D. Reynolds, Measuring hydraulic conductivity in a cracking clay soil using the guelph permeameter, Trans. ASAE 42 (4) (1999) 957–964.
[25] L. Lassabatere, R. Angulo-Jaramillo, J.M.S. Ugalde, R. Cuenca, I. Braud, R. Haverkamp, Beerkan estimation of soil transfer parameters through infiltration experiments - BEST, Soil Sci. Soc. Am. J. 70 (2) (2006) 521–532.
[26] R. Haverkamp, P.J. Ross, K.R.J. Smettem, J.Y. Parlange, 3-Dimensional analysis of infiltration from the disc infiltrometer .2. Physically-based infiltration equation, Water Resour. Res. 30 (11) (1994) 2931–2935.
[27] M.R. Abou Najm, R.D. Stewart, S. Di Prima, L. Lassabatere, A simple correction term to model infiltration in water-repellent soils, Water Resour. Res. 57 (2) (2021), e2020WR028539.
[28] P. Concialdi, S. Di Prima, H.M. Bhanderi, R.D. Stewart, M.R. Abou Najm, M. Lal Gaur, R. Angulo-Jaramillo, L. Lassabatere, An open-source instrumentation package for intensive soil hydraulic characterization, J. Hydrol. 582 (2020), 124492.
[29] S.M. Beatty, J.E. Smith, Infiltration of water and ethanol solutions in water repellent post wildfire soils, J. Hydrol. 514 (0) (2014) 233–248.
[30] A.K. Leung, A. Garg, J.L. Coo, C.W.W. Ng, B.C.H. Hau, Effects of the roots of Cynodon dactylon and Schefflera heptaphylla on water infiltration rate and soil hydraulic conductivity, Hydrol. Process. 29 (15) (2015) 3342–3354.
[31] S.H. Doerr, R.A. Shakesby, R.P.D. Walsh, Soil water repellency: its causes, characteristics and hydro-geomorphological significance, Earth Sci. Rev. 51 (1–4) (2000) 33–65.
[32] M. Iovino, P. Pekárová, P.D. Hallett, J. Pekár, Ľ. Lichner, J. Mataix-Solera, V. Alagna, R. Walsh, A. Raffan, K. Schacht, M. Rodný, Extent and persistence of soil water repellency induced by pines in different geographic regions, J. Hydrol. Hydromechanics 66 (4) (2018) 360.
[33] P. Scholl, D. Leitner, G. Kammerer, W. Loiskandl, H.P. Kaul, G. Bodner, Root induced changes of effective 1D hydraulic properties in a soil column, Plant Soil 381 (1) (2014) 193–213.
[34] P. Nyman, G. Sheridan, P.N.J. Lane, Synergistic effects of water repellency and macropore flow on the hydraulic conductivity of a burned forest soil, south-east Australia, Hydrol. Process. 24 (20) (2010) 2871–2887.